

UNITY POWER FACTOR CORRECTION CIRCUIT BASED ON BOOST-BUCK DC-TO-DC CONVERTER WITH COUPLED INDUCTANCE

Miro Milanović, Franc Mihalič, Karel Jezernik, Danilo Zadravec,
Alenka Planinc, Uroš Milutinović

KEYWORDS: power electronics, power factor correction, DC-TO-DC converters, coupled inductance, single phase circuits

ABSTRACT: The Unity power factor correction circuits are nowadays becoming one of the most important requirements for all power electronic rectifiers (equipment). The idea of using coupled inductance in a single phase diode rectifier power factor correction circuits and the influence of the coupling factor on the current ripple will be discussed in this paper.

VEZJE ZA KOREKCIJO FAKTORJA MOČI ZASNOVANO NA BOOST-BUCK ENOSMERNEM PRESMERNIKU S SKLOPLJENO INDUKTIVNOSTJO

KLJUČNE BESEDE: močnostna elektronika, korekcija faktorja moči, enosmerniki presmerniki, sklopljena induktivnost, enofazna vezja

POVZETEK: Vezja za korekcijo faktorja moči postajajo vse pomembnejši sestavni del vseh naprav močnostne elektronike. V članku bo obdelano vezje za korekcijo faktorja moči z uporabo sklopljenih induktivnosti, prav tako bo raziskan vpliv faktorja sklopljenosti na valovitost toka.

INTRODUCTION

Switch-mode power supplies, DC-AC converters for motor drive, (5, 8) require an AC-DC bridge rectifier, with a large filter capacitor. The capacitor is needed to give the specified output voltage ripple and to provide energy storage. Since the capacitor draws line current only when the output voltage is below the line voltage, the line current pulsates. This pulsating current causes a low power factor. Power supplies with such rectification have less than 0.65 power factor (Fig. 1).

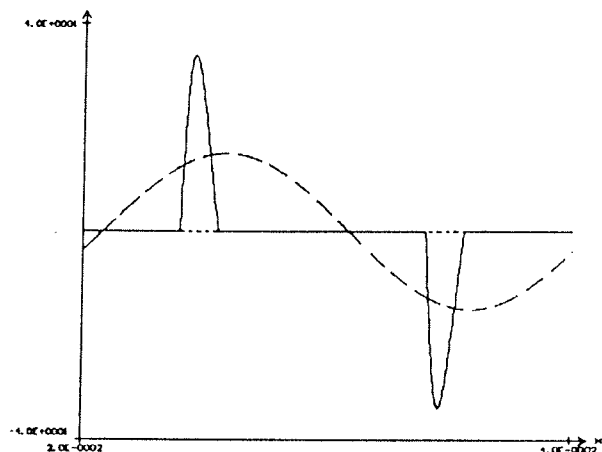


Fig. 1: Input current waveform

Using the Fourier analysis, the line current can be expressed in terms of its fundamental frequency component i_{s1} (shown by the dashed line in Fig. 1) plus the other harmonic components. If v_s is assumed to be purely sinusoidal, only i_{s1} contributes to the average power flow (2). In terms of the rms voltage V_s and the rms current I_{s1} of the fundamental frequency component of i_s , the average power P , flowing through the rectifier, is:

$$P = V_s I_{s1} \cos \Phi_1 \quad (1)$$

where Φ_1 is the phase shift between i_{s1} and V_s . The magnitude of the apparent power S is:

$$S = V_s I_s \quad (2)$$

and the power factor is defined as:

$$PF = \frac{P}{S} = \frac{I_{s1}}{I_s} \cos \Phi_1 \quad (3)$$

From eq. (3), it can be noted that a large distortion in the line current will result in a small value of the current ratio I_{s1}/I_s , and hence, a small value of PF, even if $\cos \Phi_1$ is close to unity.

The unity power factor, ie. the current ratio I_{s1}/I_s and $\cos \Phi_1$ are close to unity, can be achieved by the introduction of a high power factor correction circuits (HPFCC) (7).

The choice of power electronic converters is based on the following considerations:

- In general, for HPFC circuits, electrical isolation between the utility input and the output of the circuit is not strictly required
- In most applications, it is acceptable and in many cases desirable to stabilize the DC voltage V_d slightly higher than the maximum peak of the AC input voltage.
- Cost, power loss and size of the current shaping circuits should be as small as possible.

From the set of different available HPFC circuits for power factor correction, the boost-buck converter is chosen to be discussed.

THE PROPOSED CIRCUIT

The proposed circuit for current shaping shown in Fig. 2 consists of a boost converter connected to the line, and a buck converter connected to the output capacitor.

The boost part of the circuit, appropriately controlled, forces the input current to be sinusoidal and in phase with the input voltage (5). Relatively high amount of input current ripple is caused by the switching frequency and depends on the value of the used inductance. It will be shown that the current ripple can be significantly reduced using the effect of inductance coupling. Filtering of the input current ripple is accomplished by the buck part

of the circuit. The coupled inductance for zero current ripple in DC-DC converters was introduced by Čuk and Middlebrook (3,4).

Before describing how the current ripple can be reduced by inductance coupling, the state space equations of cascade boost-buck converter will be reviewed.

For the two switch states (ON, OFF), the circuit operation shown in Fig.11 can be described by a set of linear time-invariant differential equations:

$$\dot{x} = A_1 x + b_1 v_g \quad \text{during } dT_s \quad (4)$$

$$y_1 = C_1 x$$

and

$$\dot{x} = A_2 x + b_2 v_g \quad \text{during } (1-d)T_s \quad (5)$$

$$y_2 = C_2 x$$

where:

$$x = \begin{pmatrix} i_{L1} & i_{L2} & u_{C1} & u_{C2} \end{pmatrix}^T; \quad v_g = v_{in}$$

$$A_1 = \begin{pmatrix} 0 & 0 & -\frac{L_m}{L_1 L_2 - L_m^2} & \frac{L_m}{L_1 L_2 - L_m^2} \\ 0 & 0 & \frac{L_1}{L_1 L_2 - L_m^2} & -\frac{L_1}{L_1 L_2 - L_m^2} \\ \frac{1}{C_1} & -\frac{1}{C_2} & -\frac{1}{R_L C_1} & 0 \\ 0 & -\frac{1}{C_2} & 0 & 0 \end{pmatrix}$$

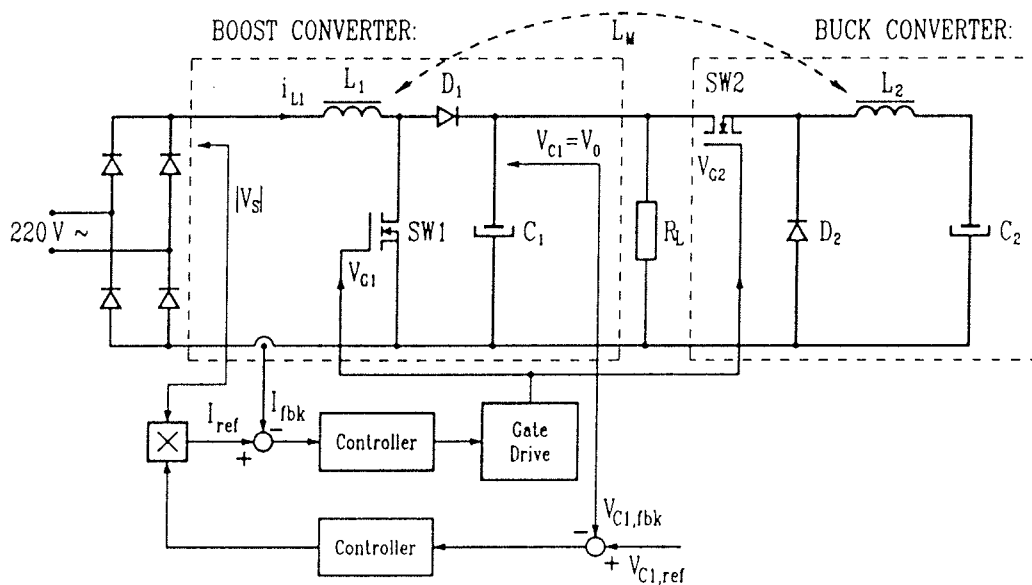


Fig.2: Boost-buck with coupled inductance

$$b_1 = b_2 = \begin{pmatrix} \frac{L_2}{L_1 L_2 - L_m^2} \\ \frac{L_m}{L_1 L_2 - L_m^2} \\ 0 \\ 0 \end{pmatrix}$$

$$A_2 = \begin{pmatrix} 0 & 0 & -\frac{L_2}{L_1 L_2 - L_m^2} & \frac{L_m}{L_1 L_2 - L_m^2} \\ 0 & 0 & \frac{L_m}{L_1 L_2 - L_m^2} & -\frac{L_1}{L_1 L_2 - L_m^2} \\ \frac{1}{C_1} & 0 & -\frac{1}{R_L C_1} & 0 \\ 0 & \frac{1}{C_2} & 0 & 0 \end{pmatrix}$$

The operation of the boost-buck converter with coupled inductance is based on a very simple principle. During the ON time input current flow only through the inductance L_1 (Fig. 3a).

The slope of the inductance current di_{L1}/dt depends on the input line voltage. By introducing the opposite voltage source V_{OPP} (Fig. 3b), this slope can be reduced (Fig. 4).

Voltage V_{OPP} is due to the introduction of a buck converter and a coupled inductance between L_1 and L_2 (Fig. 5).

The slope of the inductance current can be determined from equation (4).

$$\left. \frac{di_{L1}}{dt} \right|_{ON} = \frac{L_m}{L_1 L_2 - L_m^2} (v_{C1} - v_{C2}) + \frac{L_m}{L_1 L_2 - L_m^2} v_{in} \quad (6)$$

After making the following substitutions:

$$L_m = k\sqrt{L_1 L_2}$$

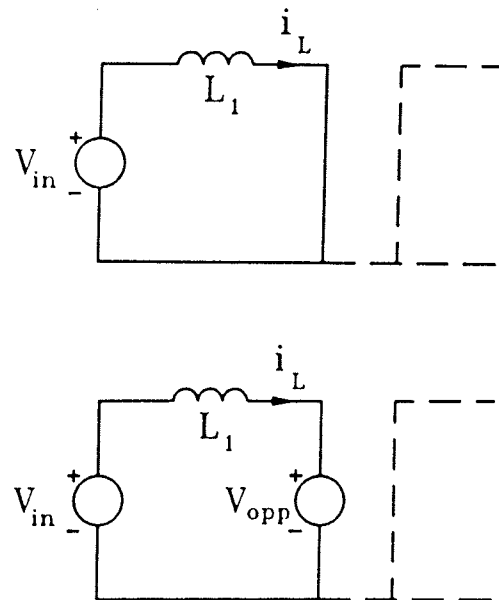


Fig. 3a,b

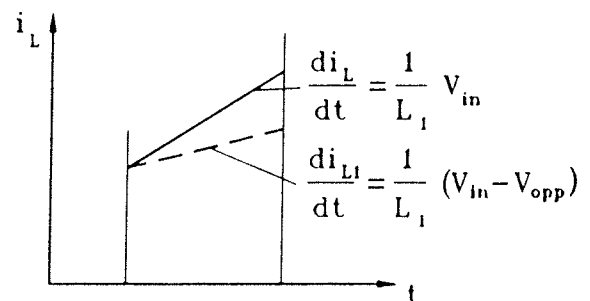


Fig. 4

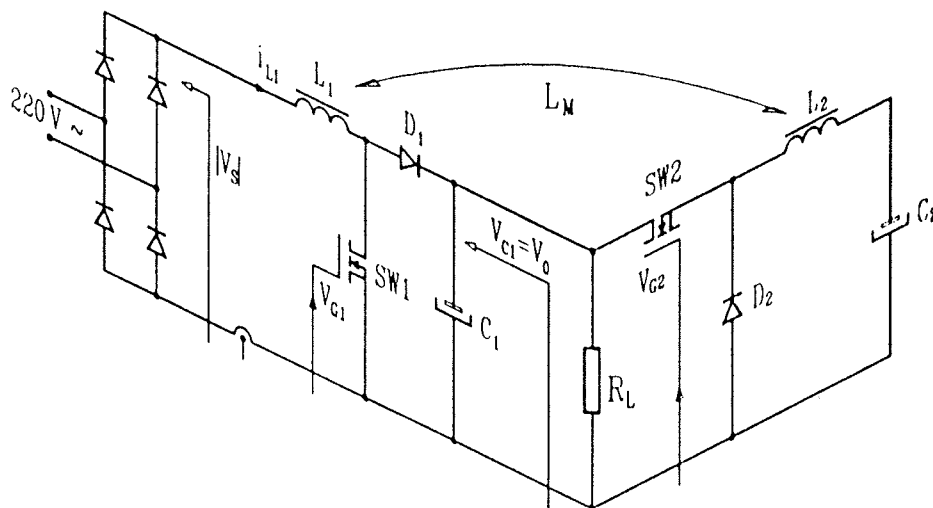


Fig. 5

$$L_1 = L_2$$

$$V_0 = V_{c1}$$

$$V_{c2} = d V_0 \quad (\text{buck-converter})$$

$$V_0 = \frac{1}{1-d} \bar{V}_{in} \quad (\text{boost-converter})$$

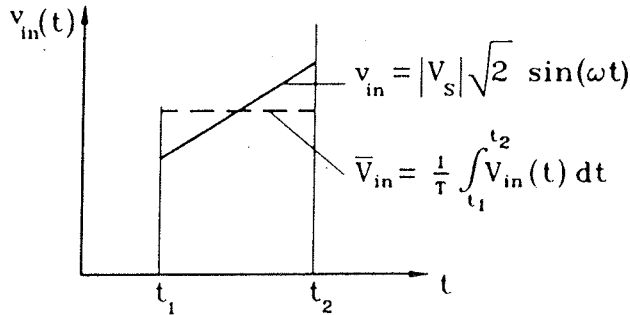


Fig.6

and rearranging, the final equation is obtained:

$$\left. \frac{di_{L1}}{dt} \right|_{ON} = \frac{1}{L_1} \frac{v_{in} - k \bar{V}_{in}}{1 - k^2} \quad (7)$$

Generally, it is desired that the slope di_{L1}/dt decreases as the coupled factor k increases. By the well-known theorems of mathematical analysis, it will hold true when k satisfies the following inequality:

$$\frac{d}{dk} \left(\left. \frac{di_{L1}}{dt} \right|_{ON} \right) = -\frac{1}{L_1} \frac{k^2 \bar{V}_{in} - 2k v_{in} + \bar{V}_{in}}{(1 - k^2)^2} \leq 0 \quad (8)$$

Since the denominator of inequality (8) is always greater than 0, the inequality is equivalent to:

$$k^2 \bar{V}_{in} - 2k v_{in} + \bar{V}_{in} \leq 0 \quad (9)$$

The discriminant of the quadratic inequality (9) is equal to $4(v_{in}^2 - \bar{V}_{in}^2)$. Therefore, all values of k satisfy (9) if $v_{in} \leq \bar{V}_{in}$. If $v_{in} > \bar{V}_{in}$, the equality $k^2 \bar{V}_{in} - 2k v_{in} + \bar{V}_{in} = 0$ has two real solutions

$$k_{1,2} = \frac{v_{in}}{\bar{V}_{in}} \pm \sqrt{\left(\frac{v_{in}}{\bar{V}_{in}} \right)^2 - 1} \quad (10)$$

and since

$$0 < \frac{v_{in}}{\bar{V}_{in}} - \sqrt{\left(\frac{v_{in}}{\bar{V}_{in}} \right)^2 - 1} < 1 < \frac{v_{in}}{\bar{V}_{in}} + \sqrt{\left(\frac{v_{in}}{\bar{V}_{in}} \right)^2 - 1} \quad (11)$$

Inequality (9) is satisfied by all k in the range

$$\left[0, \frac{v_{in}}{\bar{V}_{in}} - \sqrt{\left(\frac{v_{in}}{\bar{V}_{in}} \right)^2 - 1} \right]$$

and is not satisfied by k in the range

$$\left(\frac{v_{in}}{\bar{V}_{in}} - \sqrt{\left(\frac{v_{in}}{\bar{V}_{in}} \right)^2 - 1}, 1 \right)$$

Using notation (12):

$$\lambda = \frac{V_{in}}{\bar{V}_{in}}, \quad k_{max} = \lambda - \sqrt{\lambda^2 - 1} \quad (12)$$

the range of solutions of (9) (0,1) is further restricted to $[0, k_{max}]$. If $k \notin [0, k_{max}]$, the theorem as well as the experiment show that the slope of the current increases uncontrollably.

SMALL SIGNAL ANALYSIS

In order to shape the input current of the boost-buck converter, it must operate under the current-mode control (Fig. 7).

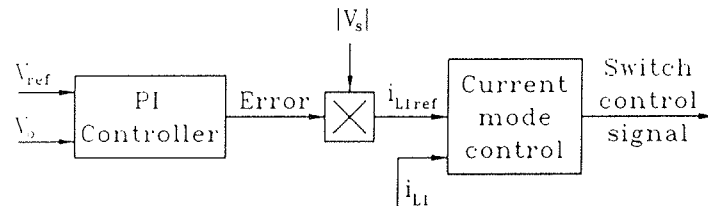


Fig.7

Once i_{L1ref} and i_L are available, there are various methods to implement the current mode control of the boost-buck converter. In this section, the constant frequency control is described in details.

The transfer function \tilde{i}_o/\tilde{d} can be obtained by the following procedure (1,2). The description of the average state-space model is given below:

$$\left. \frac{di_{L1}}{dt} \right|_{ON} = \frac{L_2}{L_1 L_2 - L_m^2} v_{in} + \frac{L_m}{L_1 L_2 - L_m^2} v_{in} (v_{c2} - v_{c1}) \quad (13)$$

$$\left. \frac{di_{L1}}{dt} \right|_{OFF} = \frac{L_2}{L_1 L_2 - L_m^2} (v_{in} - v_{c1}) + \frac{L_m}{L_1 L_2 - L_m^2} v_{c2} \quad (14)$$

The average state-space model is obtained as the sum of equations (13) and (14), after they are multiplied by d and $(1-d)$ respectively.

$$\left. \frac{di_{L1}}{dt} \right|_{ON-OFF} = \frac{L_2}{L_1 L_2 - L_m^2} (v_{in} - v_{c1} + v_{c1}d) + \frac{L_m}{L_1 L_2 - L_m^2} (v_{c1}d + v_{c2}) \quad (15)$$

By introducing small signal perturbations in (15):

$$\begin{aligned} i_{L1} &= I_{L1} + \tilde{i}_{L1} \\ v_{in} &= V_{in} + \tilde{v}_{in} \\ v_{c1} &= V_{c1} + \tilde{v}_{c1} \\ v_{c2} &= V_{c2} + \tilde{v}_{c2} \\ d &= D + \tilde{d} \end{aligned} \quad (16)$$

and considering that $\tilde{v}_{in} = 0$, $\tilde{v}_{c1} = 0$ and $\tilde{v}_{c2} = 0$, AC and DC components of (15) can be separated as follows:

$$\frac{d\tilde{i}_{L1}}{dt} = \frac{L_2}{L_1 L_2 - L_m^2} (V_{in} - (1-d) V_{c1}) - \frac{L_m}{L_1 L_2 - L_m^2} (V_{c1} D - V_{c2}) \quad (17)$$

$$\frac{d\tilde{i}_{L1}}{dt} = \left(\frac{L_2}{L_1 L_2 - L_m^2} - \frac{L_m}{L_1 L_2 - L_m^2} \right) V_{c1} \tilde{d} \quad (18)$$

The transfer function \tilde{i}_{L1}/\tilde{d} can be obtained by applying Laplace Transformations on eq. (18) and considering $V_{c1} = V_0$.

$$\frac{\tilde{i}_{L1}(s)}{\tilde{d}(s)} = \frac{L_2 - L_m}{L_1 L_2 - L_m^2} \frac{1}{s} V_0 \quad (19)$$

After substituting $L_m = k\sqrt{L_1 L_2}$ and $n = \sqrt{L_1/L_2}$ in the upper equation, the transfer function becomes:

$$G_{id} = \frac{\tilde{i}_{L1}(s)}{\tilde{d}(s)} = \frac{V_0}{L_1} \frac{1 - kn}{1 - k^2} \frac{1}{s} \quad (20)$$

Fig. 8 shows the Bode plots of the transfer function expressed by (20).

In order to obtain the voltage transfer function, the following procedure can be used: the inductance current flows through the 'rest' of the filter (Fig.9)

For the circuit shown in Fig.9 system of equations (21) can be obtained:

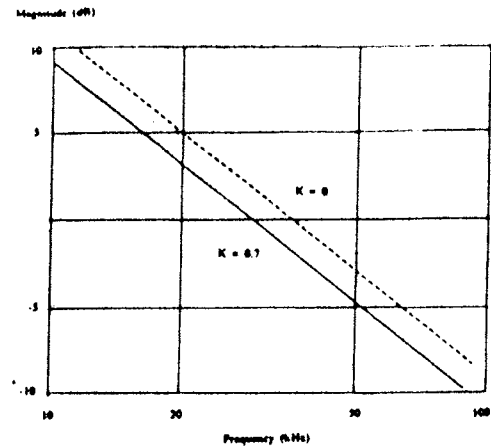


Fig.8

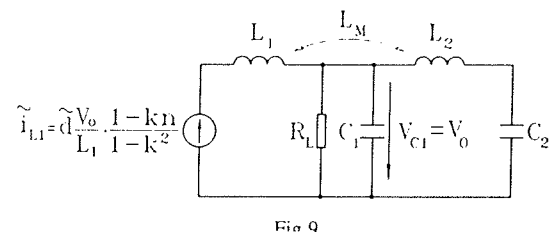


Fig.9

Fig.9

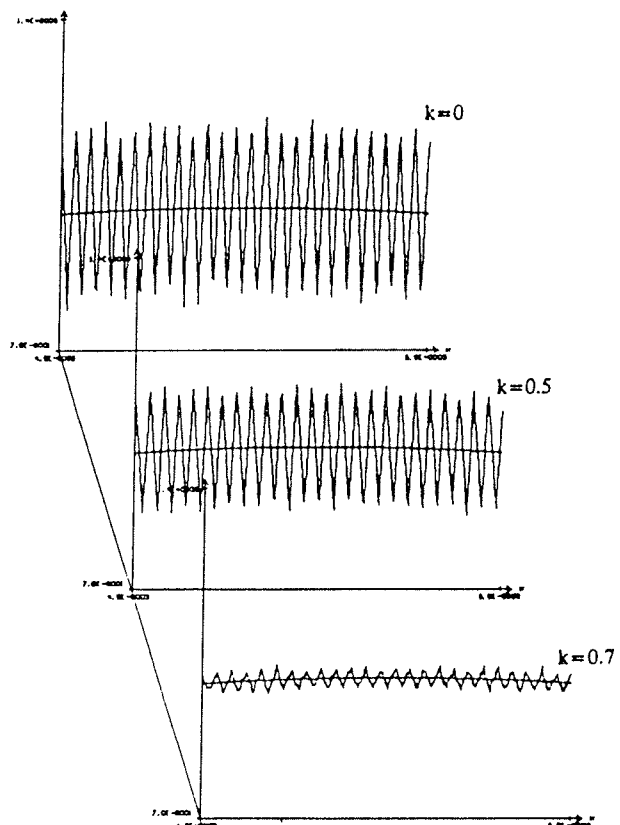
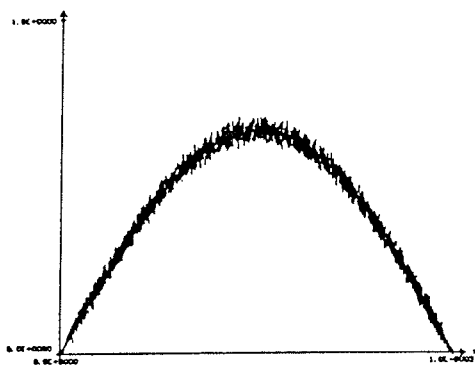


Fig. 10a,b,c,d

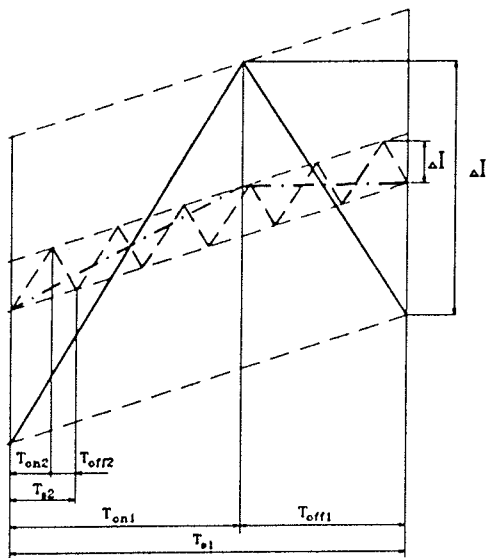


Fig. 11

$$\begin{aligned}\tilde{i}_{L1} &= C_1 \frac{d\tilde{v}_{C1}}{dt} + \frac{1}{R_L} \tilde{v}_{C1} + \tilde{i}_{L2} \\ \tilde{v}_{C1} &= L_2 \frac{d\tilde{i}_{L2}}{dt} + L_m \frac{d\tilde{i}_{L1}}{dt} + \tilde{v}_{C2} \\ \tilde{i}_{L2} &= C_2 \frac{d\tilde{v}_{C2}}{dt}\end{aligned}\quad (21)$$

The transfer function can be determined by using (21).

$$G_{vi} = \frac{\tilde{v}_o(s)}{\tilde{i}_{L1}(s)} = \frac{R_1(s^2 L_2 C_2 + s L_m + 1)}{s^3 (R_1 C_1 L_2 C_2) + (L_2 C_2) s^2 + 1} \quad (22)$$

The transfer function $v_o(s)/i_{ref}(s)$ is needed for the voltage control design.

$$G_v = \frac{\tilde{v}_o(s)}{\tilde{i}_{ref}(s)} = \frac{G_{vi} G_{id}}{1 + G_{id}} \quad (23)$$

By dividing the control problem into two parts, it is possible to shape the inductance current (line current) and control the output voltage.

SIMULATION RESULTS

Fig. 10 a,b,c and d show the simulation results for half a line period (10ms) and a part of the line current. The current ripple is reduced by factor 7.5. It is very important to note that the sampling frequency is the same in all cases.

The same ripple can be achieved if the sampling frequency is increased by a factor equal to the reduction factor of the line current ripple (Fig. 11). With coupled inductance, the power loss increases by 2 folds while with the increase of sampling frequency, it increases by factor 7.5. The sensitivity of the system to the component value variations was checked by simulation. If the component value varies for 10%, the performance is quite satisfactory.

CONCLUSION

The goal of current ripple reduction with the coupled inductance lies behind reduction of power loss. In comparison with current ripple reduction by increasing the switching frequency (Fig. 2), the proposed circuit proves to be far superior. By using the Ćuk and Middlebrook optimal topology of DC-DC converter circuit for active waveshaping interface Š3Ć, even a better result can be achieved since only one switching element would be needed.

REFERENCES

- (1) N. Mohan et al, Sinusoidal Line Current Rectification with a 100 kHz B-sit Step up Converter. PESC 1984.
- (2) N. Mohan, T. Undeland & W. Robins, Power Electronics Converters, Applications and Design; John Wiley & Sons, New York 1989.
- (3) S. Ćuk, Switching DC to DC Converter with zero input or output Current Ripple. Proceedings of IEEE Industry Applications Society Annual Meeting, October 1978, Toronto.
- (4) S. Ćuk, R.D. Middlebrook, Coupled Inductor and Other Extensions of a New Optimum Topology Switching DC to DC Converter, IEEE Industry Applications Society Annual Meeting 1977.
- (5) C. Zhou, R.B. Ridley, F.C. Lee, Design and Analysis of an Active Unity Power Factor Correction Circuit, Proceedings VPEC, Blacksburg VA, 1988.
- (6) M. Kazerani et al, Programable input power factor correction methods for single phase diode rectifier circuits APEC, LA 1990.
- (7) R. White, M. Sayani, High Power Factor AC-DC converters, Professional Education Seminars Workbook, APEC '90, L. A., CA, March 11-16, 1990, pp. 1-52.
- (8) F. Mihalič, M. Milanović and K. Jezernik, Unity Power Factor Rectification for an AC Motor Drive, IEEE Melecon '91, Ljubljana 1991, SLO, Proceedings Volume II, pp. 1421-1424.

Miro Milanović, Franc Mihalič, Karel Jezernik, Danilo Zdravec, Alenka Planinc, Uroš Milutinović*

University of Maribor Faculty of Technical Sciences
Smetanova 17
62000 Maribor, Slovenia

*Faculty of Education
Koroška cesta 160
62000 Maribor, Slovenia